Essential Readings in Light Metals: Aluminum Reduction Technology.
Edited by Geoff Bearne, Marc Dupuis and Gary Tarcy.

On the anode effect in aluminum electrolysis

J. Thonstad[1], T.A. Utigard[2] and H.Vogt[3]
[1]Norwegian University of Science and Technology, Trondheim, Norway;
[2]University of Toronto, 184 College Street, Toronto, Ontario, Canada, M5S 3E4;
[3]University of Applied Sciences, D-13353, Berlin, Germany

Abstract

Anode effects are detrimental in that they result in reduced energy efficiency and cause emissions of CF_4 and C_2F_6. With prospects of future CO_2 taxes, the emissions of these greenhouse gases may become costly. With a CO_2 tax of 15 US$ per tonne, each anode effect minute per day per cell will increase the production cost by about 1.2%. Research work related to anode effects has been reviewed and analyzed. The wetting of the anode deteriorates as the alumina content decreases, leading to increased gas coverage of the base of the anode. With decreasing effective surface area, the actual current density increases. Anode effects then occur when the alumina content becomes too low and the local current density exceeds the critical current density. The paper concludes by analyzing various methods that may be used to decrease the frequency and duration of anode effects in prebake as well as Soderberg cells.

Introduction

In industrial cells anode effects (AE) occur when the bath alumina content becomes too low to maintain normal electrolysis. The cell voltage rises abruptly to 20 - 50 V leading to over-heating of the cell and meltback of the side-ledge. More detrimental are the significant emissions of CF_4 and C_2F_6. Both are powerful greenhouse gases and have long lifetimes in the atmosphere (10^4 – 10^6 years). The so-called "global warming potential" which is related to that of CO_2, is 6500 for CF_4 and 9200 for C_2F_6 [1]. This implies that CF_4 is 6500 times more powerful as a greenhouse gas than CO_2. To reduce the emissions of these gases, the aluminium industry has made significant improvements in decreasing the duration and frequency of anode effects. This has been achieved by improved feeding of alumina and control of its content in the bath. However, as seen in Fig. 1 [2], anode effects contribute significantly to the overall greenhouse gas emissions, in particular from Soderberg cells. With proposed greenhouse taxes, these emissions may lead to significant increases in operating costs.

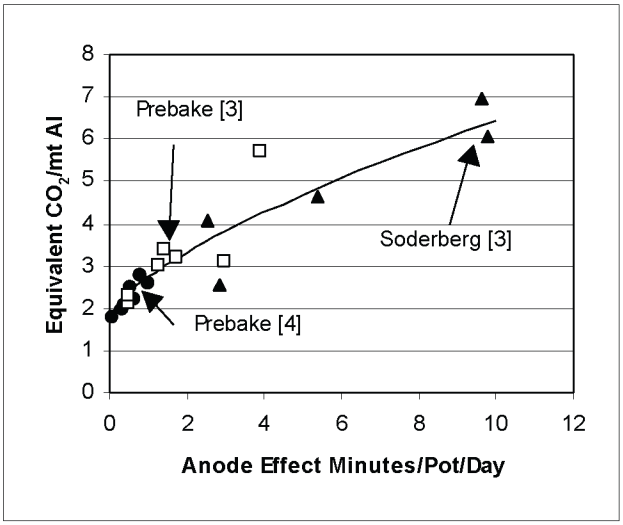

Figure 1. Equivalent CO_2 emissions versus AE minutes/day [2].

Critical Current Density

The tendency for a given bath to provoke AE is expressed by the critical current density (ccd), which is the maximum current density before AE is initiated. As seen in Fig. 2, laboratory experiments show that the ccd increases with increasing alumina content, from 0.1 A/cm^2 in pure cryolite to more than 20 A/cm^2 in alumina-rich melts [5-7]. Qiu et al. [8-10] found that anodes which previously had undergone an AE, showed lower ccd, indicating a memory effect on the anode providing evidence for certain physical or chemical changes taking place at the surface of the anode.

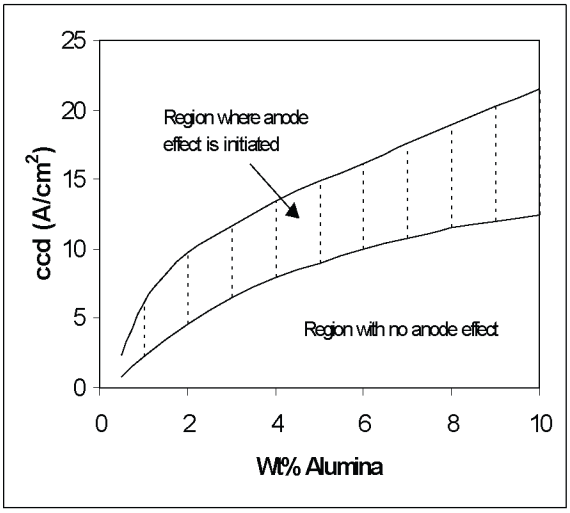

Figure 2. Critical current density versus alumina content for laboratory cells [5].

Voltammetric Investigations

Voltammetric studies are carried out by recording the current as a function of the voltage. Figure 3 gives a typical current-voltage behavior during AE [14-16]. After exceeding the ccd, the potential will normally jump to the 25 - 45 V range which is a normal AE voltage. Soderberg cells may experience AE voltages up to about 60 – 80 V while 'sick' prebake cells may have AE voltages as low as 15 V.

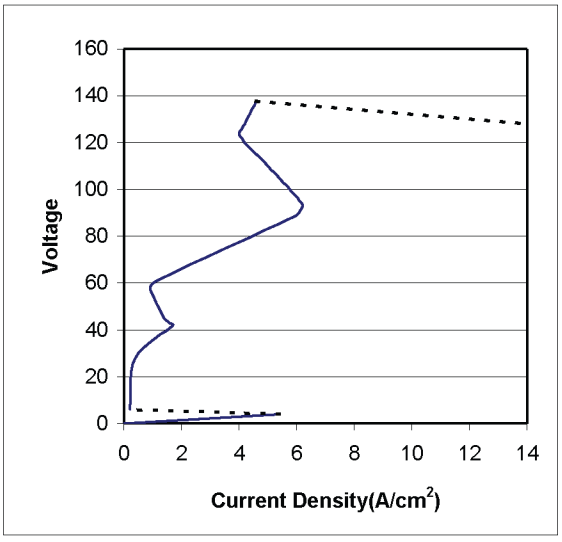

Figure 3. Current-voltage diagram during AE in a laboratory cell [14].

In a laboratory investigation with variously shaped anodes, Popelar et al. [17] obtained results similar to those shown in Fig. 3. In the voltage range below 55 V it was found that anodes with a rough surface carried more current than anodes with smooth surfaces.

At slow sweep rates and low alumina contents (< 1.3 wt% Al_2O_3) two distinct current peaks are observed as the voltage is increased. The first peak is assigned to CO_2 and the second to CF_4 [11]. At high alumina contents the CO_2 peak dominates, representing the critical current density (ccd) of the system. At high sweep rates (> 20 V/s) a new peak appears between the CO_2 and CF_4 peaks as seen in Fig. 4. Calandra et al. [11-13] attributed this peak to COF_2 formation.

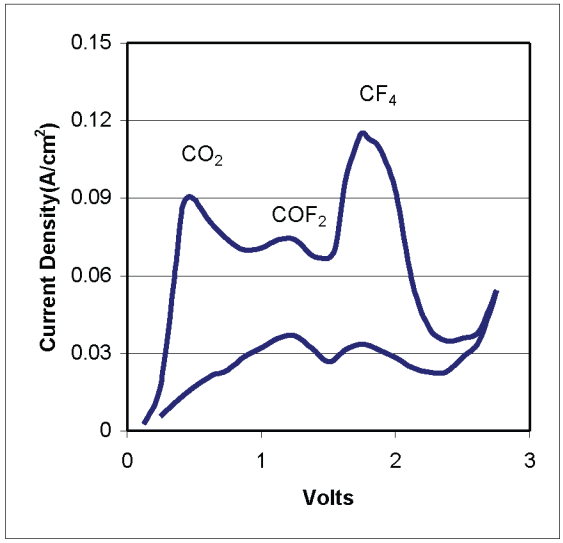

Figure 4. Voltammetric curves obtained at a sweep rate of 80 V/s [11-13].

Although not found in the laboratory experiments by Zhu and Sadoway [18], Dorreen et al. [19] detected the gaseous species COF_2 actually a few minutes before the AE occurred. The formation reaction could be,

$2/3\ Na_3AlF_6 + 1/3\ Al_2O_3 + C = 4/3\ Al + 2\ NaF + COF_2;$ $E° = -1.83$ V at 1000 °C

COF_2 can also be formed by reactions such as

$$CF_4(g) + CO_2(g) = 2COF_2(g);$$
$$K_{eq} = 1.16 \text{ at } 1000\ °C$$

$$CF_4(g) + 2CO(g) = 2COF_2(g) + C(anode);$$
$$K_{eq} = 0.009 \text{ at } 1000\ °C$$

'Visual' Observations

Noguchi et al. [20] studied the AE by "the hot thermocouple method" where a 5 mg droplet of cryolite was heated in a see-through cell and touched by graphite electrodes. During normal electrolysis individual gas bubbles could be seen leaving the anode while when AE set in, the current dropped from 300 to 40 mA and the anode became covered by a gas film and sparks appeared. Qiu et al. [8-10] used a see-through cell with a drop of cryolite resting on a graphite plate and with a graphite anode dipped into it. The anode became non-wetting during AE and sparks were seen. Similar observations were made in a see-through cell made of quartz [21] where it was observed that the entire anode was covered with a continuous layer of gas.

Utigard et al. [22, 23] used an X-ray radiographic method to observe the interior of a graphite crucible containing a cryolite melt and a graphite anode (2-9 mm dia.). During normal electrolysis in alumina-containing melts, one large bubble would grow at the base of the anode, while several smaller bubbles grew and became detached from the vertical side of the anode. The AE was provoked using a high purity cryolite melt, and the AE then occurred at 2.6 V without any prior gas evolution [23]. The anode became totally non-wetted by the electrolyte and it became separated from the anode. Due to surface tension forces, gas from above the melt was sucked rapidly down along the sides of the anode to form a gas bubble beneath the bottom of the anode. Any gas subsequently produced at the anode escaped through this film without forming bubbles. The film was 3 mm thick at the base and it was calculated to be about ~3 μm up along the sides.

Passing gases (Ar, H_2-N_2, CF_4, CO_2) through a hole in the anode during AE had no effect on the gas film. It is interesting to note that CF_4 gas had absolutely no effect on the gas behavior either during normal electrolysis or during anode effects. The same authors [22] also studied AE using a hot stage microscope with a 1 mm diameter graphite anode. During AE the electrolyte was found to be completely non-wetting with respect to the anode.

Mechanism of the Anode Effect

In cryolite with almost no Al_2O_3, in the laboratory AE can be initiated with a current pulse that corresponds to the formation of only a few monolayers. Thonstad et al. [14] calculated that the initiation of AE corresponds to the charging of a condenser. This was supported by Utigard et al. [23] who showed that in pure cryolite AE could be initiated with no prior gas evolution.

The other extreme occurs on gold or platinum anodes where it is necessary to reach current densities above 50 A/cm^2 to initiate AE [24, 25]. Under such conditions of extreme gas evolution rates (13 cm^3/cm^2·s or 13 cm/s), the gas may prevent the electrolyte from contacting the electrode, leading to increased voltage and ionization of the gas. This hydrodynamic initiation mechanism is different from that with carbon anodes in 'pure' cryolite with minimal gas evolution. In industrial cells it is expected that both mechanisms are involved in the initiation of an AE.

In industrial cells, anode effects are normally initiated for alumina contents between 0.5 and 2.2 wt% [5]. From the graph in Fig. 2, which is based on laboratory data, the critical current density should for these alumina contents be somewhere between 1 and 10 A/cm^2, which is higher than the anodic current density in industrial cells (0.6-0.8 A/cm^2). This shows that in industrial cells with large anodes, anode effects are initiated at lower average current densities than those in laboratory cells, suggesting that for large anodes the gas coverage of the anode may play a very important role.

In a typical industrial cell with a current density of 0.7 A/cm^2, the gas generation corresponds to a gas formation velocity of 0.2 cm/s (0.2 cm^3/cm^2·s). Due to surface tension forces the bubble penetration depth beneath the anode is about 0.5 cm [26]. Since more than 20% of the surface of the anode bottom is covered by gas bubbles at any point in time [27], the average residence time of gas beneath an anode can be no more than 2 seconds. In particular for Soderberg cells this means that the gas has to flow at a fairly high velocity (0.5 to 2 m/s) along the bottom surface of the anode before it can escape.

The size and the flow of the gas bubbles are controlled by the size and tilt of the anode, the cell current, contact angle between the bath and the anode, surface tension of the bath and drag forces due to the moving liquid. As the gas moves horizontally, individual bubbles touch and coalesce, forming large gas bubbles that can blanket large areas of the anode. Vogt [28-30] used surface tension and wetting data to develop a hydrodynamic model to predict the onset of AE. As the alumina content decreases, the wetting of the anode gradually becomes worse and the gas bubbles tend to spread out more. The decreasing wetting also decreases the gas penetration depth into the bath, leading to a reduced bubble release velocity beneath the anodes. Together these factors increase the gas coverage and decrease the active surface area for electrolysis.

With decreasing effective surface area available for electrolysis, the actual local current density increases. The diffusion overvoltage increases and as long as alumina is not added, the cell inevitably drifts toward AE. The calculations by Vogt [28-30] predict that under industrial conditions, the onset of AE occurs when nearly 99% of the anode is covered by gas bubbles. This is in general agreement with the estimates by Polyakov [31] and Richards [27] (> 80%) immediately prior to AE and it is also in close agreement with the experimental value obtained by Brunet and Mergault [32]. It must, however, be remembered that as the cell voltage gradually increases towards AE, more and more current passes through the vertical sides of the anodes. In spite of this, eventually the local critical current density is exceeded and AE is initiated.

The exact nature of the non-wetting or insulating species formed as the current density exceeds the ccd, is not known. However, most evidence suggests that adsorbed CF_x species are formed [24]. Dewing [26] pointed out that the formation of CF_4 is slow since after two F's have been discharged on to a carbon atom, the surface will be temporarily blocked. This blockage decreases further the area available for electrolysis, leading to an almost instantaneous spreading of the AE over the entire cell.

In fluorine electrolysis in a KF·2HF electrolyte it is known that the anode gets covered with a poorly conducting layer of solid carbon fluoride (CF_x), which causes AE [33-34]. At high temperatures this compound is not thermodynamically stable, but as an adsorbed surface compound it may exist. Furthermore, the voltage rise in fluorine cells is not as abrupt as in aluminium cells and the voltages are not as high (anodic overvoltage of about 3 V). This could be because the current density is only about 0.1 to 0.15 A/cm^2. Interestingly this corresponds to the highest sustainable current density for CF_4 evolution without provoking AE in a cryolite melt [35].

The see-through cell studies by Utigard et al. [22, 23] give convincing evidence that there is a gas film covering the anode during AE. However, it has been suggested [11, 22, 23] that the gas film is a secondary phenomenon and not the primary reason for the occurrence of the AE. The fact that bubbling of gases (Ar, H_2-N_2, CF_4, CO_2) through a hole in the anode during normal electrolysis as well as during AE had absolutely no effect, shows that these gases alone will not initiate an AE. This implies that the surface of the carbon anode itself becomes either non-wetting or insulating, promoting the initiation of the AE. This further supports the suggestion that the formation of adsorbed carbon fluoride(CF_x) triggers the final stage in the initiation of an AE.

Anode Effect in Industrial Cells

For industrial cells it has been found [14, 36] that the AE voltage decreases with increasing depth of immersion, going from 80 V at 10 cm to 30 V at 25 cm as illustrated in Fig. 5. Based on such and other observations, it has been suggested [36-38] that the underside of the anodes is nearly insulated during AE so that most of the current flows through the sides of the anode. Thonstad et al. [14] measured the gas pressure beneath industrial Soderberg anodes both during normal electrolysis and during AE's. During normal electrolysis it was found that the pressure fluctuated corresponding to bath level fluctuations of about 0.4-0.7 cm, probably due to gas bubble movements. At the onset of AE these fluctuations ceased. This supports laboratory work [23] which indicates that the whole anode is covered by a gas film and any gas flows out through this film without forming bubbles. This is also supported by Oganisyan [6] who concluded that during AE the anode is covered by a continuous gas film and that most of the current passes through the sides of the anode.

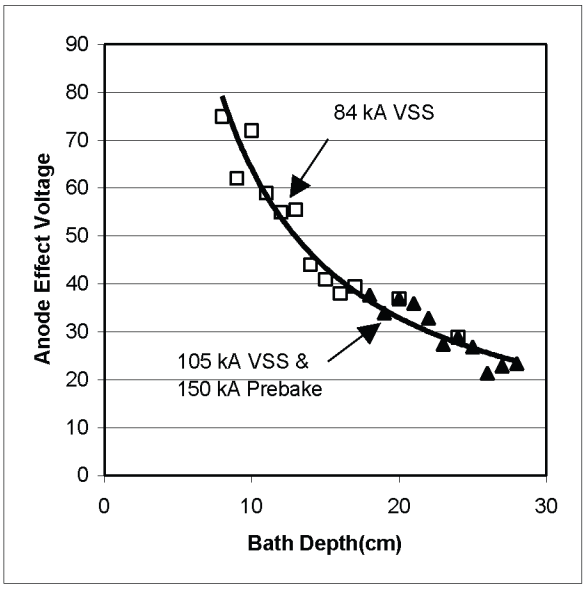

Figure 5. AE voltage versus depth of electrolyte [14].

Gaseous species. During AE the anode gas contains at least two new gaseous species, namely CF_4 and C_2F_6 [18, 19, 39, 40], which can be associated with the following reactions,

$4/3\ Na_3AlF_6 + C = 4/3\ Al + 4\ NaF + CF_4$
$E° = -2.50$ V at 1000 °C

$2\ Na_3AlF_6 + 2\ C = 2\ Al + 6\ NaF + C_2F_6$
$E° = -2.69$ V at 1000 °C

For laboratory cells Nordmo and Thonstad [41] found that the CF_4 content during AE reached 90% in very pure cryolite, and decreased sharply by the addition of small amounts of alumina, reaching about 10% at 1 wt% Al_2O_3. This is lower than that normally observed in industrial cells, typically around 15% CF_4, varying C_2F_6, 20% CO_2, with the balance CO. In industrial cells Øygård et al. [42] extracted anode gas from holes through the anodes as well as gas leaving the cell through the gas duct. It was found that undiluted anode gas extracted through the anode contained far more CF_4 than the duct gas, and it was assumed that some conversion had taken place. This conversion may be due to reactions with Al_2O_3.

In the presence of water vapor, both CF_4 and COF_2 are thermodynamically very unstable, as illustrated by the very high equilibrium constants for the following two reactions,

$$COF_2(g) + H_2O(g) = 2HF + CO_2(g);$$
$$K_{eq} = 3.7 \cdot 10^8 \text{ at } 1000\ °C$$

$$CF_4(g) + 2H_2O(g) = 4HF + CO_2(g);$$
$$K_{eq} = 1.6 \cdot 10^{17} \text{ at } 1000\ °C$$

Apart from the few laboratory observations of COF_2 and traces of CF_4 prior to AE, it is generally agreed that significant amounts of CF_4 and C_2F_6 are emitted from aluminium cells only during AE. Berge et al. [43] conducted a study in Norwegian aluminium plants and found that Soderberg cells experience on average 2.4 AE's per cell day with an average duration of 4.0 min, leading to 0.2-0.8 kg CF_4 and C_2F_6 emissions per metric tonne of aluminum. Prebake cells experience on average 0.13 AE's per cell day with an average duration of 3.8 min, leading to 0.02-0.06 kg CF_4 and C_2F_6 per metric tonne of aluminum.

Tabereaux [44] presented the data shown in Fig. 6 for an AE in an industrial prebake cell. The content of C_2F_6 goes through a peak and drops to zero after 2-3 minutes. Peak contents of C_2F_6 as low as 1% [44] and as high as 7% [42] have been recorded. Tabereaux et al. [45] found in some cases no C_2F_6 in Soderberg cells.

Leber et al. [3] reported an investigation carried out at seven US plants. The PCF emissions were found to be proportional to the duration of AE, expressed as AE minutes per cell-day. Marks [4] also reported that CF_4 emissions were proportional to the AE minutes per day, and presented the following relationship,

kg CF_4 / tonne Al = 0.13 x AE min. / cell day

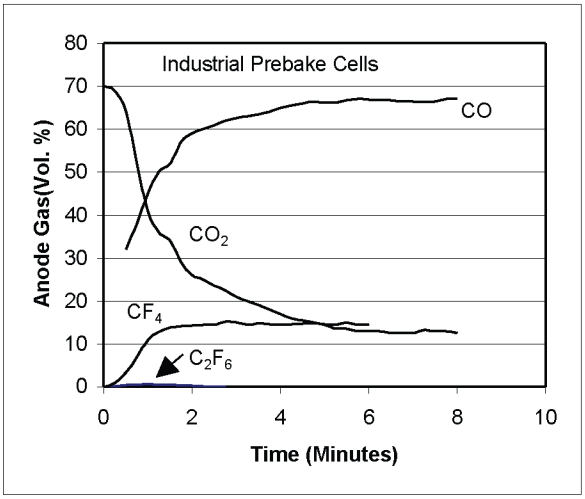

Figure 6. Gas composition in industrial prebake cells during AE [44].

In the Scandinavian countries a carbon tax has either been introduced or is being discussed. The state of Minnesota is also in the process of evaluating the effects of such a tax. The rates vary between the different countries, and industrial users usually pay less than private consumers. Reported values vary from about 7 to 40 US$ per metric tonne of CO_2 equivalent. With a tax of 15 US$ per metric tonne of CO_2 equivalent, the cost of AE becomes

Cost/ tonne Al = 12.7 US$ per AE min. / cell day

Control of Anode Effects in Industrial Cells

The old practice of using AE as a way to control the alumina content in the electrolyte is being abandoned [27] and specific programs to minimize AE's have been implemented [46-48]. AE's normally arise at alumina contents between 0.5 and 2.2 wt% Al_2O_3. There are indications that cells that are in good conditions tend to have AE at low contents (0.5-1 wt% Al_2O_3) while troubled cells may undergo AE at alumina contents above 2 wt%. Kachanovskaya et al. [49] attributed the variation in alumina contents at AE to alumina concentration gradients between the bulk of the bath and that at the anode base and to differences in gas

coverage of the anode surface.

Although the AE occurs abruptly, its pending occurrence is normally signalled in advance by a gradual increase in cell voltage as illustrated in Fig. 7. The duration and magnitude of the potential increase depend on the alumina content at which the AE occurs.

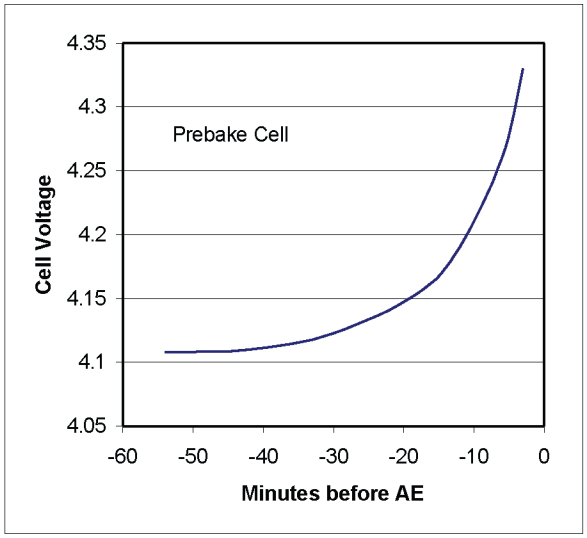

Figure 7. Voltage rise prior to an anode effect [50].

The fact that the AE does not occur at a fixed alumina content, but within a fairly wide concentration range, has complicated the use of the cell voltage for prediction of the AE. Thonstad et al. [14] found that the current distribution between the various anodes was normal 15 minutes before AE, while that this was not the case 100 seconds before AE. These variations as well as cell voltage fluctuations not connected to the alumina content, add to the complexity of predicting anode effects. In spite of these difficulties, for pre-baked cells the industry has been able to develop excellent alumina control strategies based on the fact that the cell resistance has a minimum at about 3 - 4 wt% alumina and that voltage continuously increases with further decreases in the alumina content [51-53].

Once an AE has started, a fair amount of alumina is added, in some cases after a short waiting period to raise the temperature to facilitate alumina dissolution. In addition it is necessary to stir the electrolyte. In Soderberg cells AE's are terminated manually by using wooden poles [54] or by blowing compressed air through steel tubes through the anode [55]. In prebake cells AE's are normally terminated by moving the anodes down and up in steps or by tilting the anode table [56]. Short-circuiting or shunting out a part of the cell are also effective ways of quenching an AE [47, 57].

The frequency with which the AE occurs in aluminium reduction plants varies widely, depending on the cell design, cell control and the feeding practice for alumina. Soderberg cells tend to have more than one AE per day [3], but by introduction of point feeding, this number has been reduced to 0.4-0.5 [56, 59]. For point-fed prebake cells the frequency is as low as 0.03 per day [60]. Equally important is the duration of the AE. With manual tending it can last several minutes, while with automatic control it can be brought down to 40-80 seconds [27].

Future Developments

Tabereaux [44] estimated that globally the aluminium industry annually emits 30,000 tonnes of CF_4 and 3,000 tonnes of C_2F_6, being the equivalent of 223 million tonnes of CO_2. With possible future greenhouse gas taxes of about 15 US$/tonne of CO_2, this corresponds to an added cost of 3.3 billion US$, providing great incentives for further decreasing the frequency and duration of AE's.

To improve alumina control and to decrease the frequency of AE's in Soderberg cells, Hydro Aluminum [58] and Elkem [59] have successfully introduced the use of point feeders along the sides of Soderberg cells. Utigard et al. [61, 62] have recently developed a process to inject alumina powder through lances in the anode to promote controlled and continuous alumina additions to Soderberg cells. However, this technology still has to be proven commercially.

Since CF_4 and C_2F_6 are unstable in the presence of water vapor, it may be possible during AE's to blow air rich in water vapour through lances in the anode to convert CF_4 and C_2F_6 to HF and CO_2 before the gases leave the cell. In addition, water vapour may also react with any CF_x on the anode surface quickly terminating the AE. Since there is a thin gas film covering the whole anode, the water vapour can quickly cover most of the anode underside. The water vapour may come as a low grade steam or from the combustion of natural gas leading to the formation of CO_2 and H_2O. CF_4 may also be converted in a reactor using activated Al_2O_3 as catalyst at around 700 °C in the presence of water vapour [63].

To further improve the detection of imminent AE's before they start, it may be possible to use ultrasonic or vibration sensors [64] attached to the shell of Soderberg

anodes or to individual studs. These sensors should be capable of detecting any changes to the gas bubble release and behaviour as AE is approached. Such sensors have found applications in the steel industry [65] and could become very useful in decreasing the frequency of AE's in Soderberg cells.

Conclusions

As the alumina content decreases, the wetting deteriorates and the gas coverage of the anode increases, leading to increasing local current densities. Anode effects are initiated when the local current density exceeds the critical current density. This leads to the formation of CF_x compounds at the anode causing sudden and complete non-wetting of the anode. The cell voltage increases sharply and CF_4 and C_2F_6 gases evolve.

CF_4 and C_2F_6 are greenhouse gases, and emissions of these gases may be penalized by future 'carbon' taxes. Various means of improving alumina control and preventing anode effects in Soderberg cells have been discussed.

Acknowledgement

The authors are grateful for the financial support from the Research Council of Norway.

References

1. Eyles, J., 6th Australasian Aluminium Smelter Techn. Conf. Workshop, Queenstown, New Zealand, 22-27 Nov. 1998.
2. Utigard, T.A., Light Metals 1999, 319-326.
3. Leber, B.P., Tabereaux, A.T., Marks, J., Lamb, B., Howard, T., Kantamaneni, R.,Gibbs, M., Bakshi, V. and Dolin, E.J., Light Metals 1998, 227-285.
4. Marks, J., Light Metals 1998, 287-291.
5. Grjotheim, K., Krohn, C., Malinovsky, M., Matiasovsky, K. and Thonstad, J., Aluminium Electrolysis, 2nd edition, Aluminium Verlag, 1982.
6. Oganisyan, G.L., Russ. J. Non-Ferrous Met. 36(1), 1995, 36-41.
7. Piontelli, R., Mazza, B. and Pedeferri, P., Metallurgia Ital. 57(2), 1965, 51-69.
8. Qiu, Z.-X., Wei, C.-B. and Chang, M.-J., Light Metals 1982, 279-293.
9. Qiu, Z.-X., Wei, C.-B. and You, K., Aluminium 59, 1983, 753-756.
10. Qiu, Z., Wei, Q., Yu, Y. and Fan, L., Molten Salts, Proc. 9th Int. Symp., Electrochem. Soc. 1994, 594-600.
11. Calandra, A.J., Castellano, C.E. and Ferro, C.M., Electrochim. Acta 24, 1979, 425-437.
12. Calandra, A.J., Castellano, C.E., Ferro, C.M. and Cobo, O., Light Metals 1982, 345-358.
13. Calandra, A.J., Ferro, C.M and Castellano, C.E., Electrochim. Acta 25, 1980, 201-209.
14. Thonstad, J., Nordmo, F. Husoy, A.H., Vee, K. and Austrheim, O.G., Light Metals 1984, 825-839.
15. Thonstad, J., Nordmo, F. and Vee, K., Electrochim. Acta 18, 1973, 27-32.
16. Nordmo, F. and Thonstad, J., Electrochim. Acta 29, 1984, 1257- 1262.
17. Popelar, P., Utigard, T.A. and Desclaux, P., Proc. Int. Symp.Advanc. Prod. Fabr. Light Met. Metal Matrix Comp., CIM Conference, Edmonton, Aug. 23-27, 1992, pp. 39-53.
18. Zhu, H. and Sadoway, D.R., Light Metals 1999, 241-246.
19. Dorreen, M.D.L., Chin, D.L., Hyland, M.M. and Welch, B.J., Light Metals 1998, 311-316.
20. Noguchi, F., Ueda, Y., Yanagase, T. Eran, H.G. and Kammel, R., Erzmetall, 38, 1985, 189-195.
21. Qui, Z., Fan, L. and Grjotheim, K., Aluminium 62, 1986, 341-344.
22. Utigard, T.A., Costa, H., Popelar, P., Walker, D.I., Cool, G. and Hoang, P., Light Metals 1994, 233-240.
23. Utigard, T.A., Toguri, J.M. and Ip, S.W., Light Metals 1988, 703-706.
24. Qiu, Z. and Zhang, M., Electrochim Acta 32, 1987, 607-613.
25. Dewing, E. and Kouwe, E., J., Electrochem. Soc. 124, 1977, 58-64.
26. Dewing, E., Canadian Met. Quart., 30, 1991, 153-161.
27. Richards, N.E., Light Metals 1994, 393-402.
28. Vogt, H., J. Appl. Electrochem., 29, 1999, 137-145.
29. Vogt, H., J. Appl. Electrochem., 29, 1999, 779-788.
30. Vogt, H., Electrochem. Acta, 42, 1997, 2695-2705.
31. Polyakov, P.V., Mozhaev, V.M., Burnakin, V.V, Kryukovskii, V.V, and Nikolaenko, V.E., Sov. J. Non-Ferrous Met. Res., 1, 1979, 46-52.
32. Brunet., C and Mergault, P., Rev. Inst. Hautes Temp. Refract., 20, 1983, 17-24.
33. Nicolas, F., Groult, H., Devilliers, D. and Chemla, M., Electrochimica Acta 41, 1996, 911-918.
34. Groult, H., Devilliers, D., Vogler, M., Hinnen, C, Marcus and Nicolas, F, Electrochimica Acta 38, 1993, 2413-2421.
35. Thonstad, J., Nordmo, F. and Rρdseth, J., Electrochim. Acta 19, 1974, 761.
36. Antipin, L.N. and Vazhenin, S.F., Elektrokhim. Rasplav. Solei, p. 314, Metallurgizdat, Moscow

1964.
37. Desclaux, P. and Huni, J.P.R., Light Metals 1986, 387-395.
38. Begunov, A.I., Kulikov, V.N. and Grinberg, I.S., Light Metals 1996, 369-374.
39. Henry, J.L. and Holliday, R.D., J. Metals 9, 1957, 1384-1385.
40. Holliday, R.D. and Henry, J.L., Ind. Eng. Chem. 51, 1959, 1289-1292.
41. Nordmo, F., and Thonstad, J., Electrochim. Acta 30, 1985, 741-745.
42. Øygård, A., Halvorsen, T.A., Thonstad, J., Røe, T. and Bugge, M., Light Metals 1995, 279-287.
43. Berge, I., Huglen, R., Bugge, M., Lindstrøm, J. and Røe, T., Light Metals 1994, 389-392.
44. Tabereaux, A.T., JOM 46 (11), 1994, 32-34.
45. Tabereaux, A.T., Richards, N.E. and Satchel, C.E., Light Metals 1995, 325-333.
46. Bereciartu, J., Light Metals 1986, 371-376.
47. Meyer, H.J. and Earley, D.G., Light Metals 1986, 365-370.
48. Paulsen, K.A., Mellerud, T. and Thuestad, J.G., Light Metals 1986, 377-383.
49. Kachanovskaya, I.S., Sirayev, N.S., Lebedeva, I.E., Romanov, V.P. and Kuznetsov, E.I., Sov. J. Non-Ferrous Met. 14 (4), 1973, 28-31.
50. Taylor, M.P., Welch, B.J. and Keniry, J.T., J. Electroanal. Chem., 168, 1984, 179-192.
51. Reverdy, M., 11th Int. course on process metallurgy of aluminium, NTH, Trondheim, Norway, 1992, Ch. 8, 1-81.
52. Levenig, B., Light Metals 1995, 387-389.
53. Jie, L., Yongzhong, H., Huazhang, W. and Yexiang, L., Light Metals 1994, 441-447.
54. Grjotheim, K., Kvande, H. and Qiu, Z., JOM 47 (11), 1995, 32-35.
55. Brandtsæg, S.R., Paulsen, K.A. and Thovsen, K., Light Metals 1988, 603-606.
56. Saksvikrønning, T., Valsvik, G. and Hove, S.J., Light Metals 1982, 553-557.
57. Buzunov, V.Yu., Shestakov, V.M., Polyakov, P.V., Thikhomirov, V.N. and Resmyatov, S.S., Tsvetnye Met. 35 (6), 1994, 30-33.
58. Paulsen, K.A., Rolland, W.R., Larsen, A. and Bugge, M., Light Metals 1997, 195-199.
59. Pedersen, T.B., Bentzen, H.J., Jensen, M., Larsen, W., Olsen, A.T., Pedersen, R. and Syrdal, A.K., Light Metals 1998, 221-226.
60. Hydro Aluminium, Karmoy, Norway, Private communications, July 1999.
61. Utigard, T.A, Bustos, A.A. and Dahl, T., US Patent 5,759,382, Jun. 2, 1998.
62. Utigard, T.A, Kapusta, J.P. and Bustos, A.A. , Proceedings of the International Symposium on Light Metals, Quebec City, Aug. 1999, 17-25.
63. Diep, Q.B., Thonstad, J. and Rye, K.A., ZSNP VIII Al Symposium, 25-27 Sept, 1995, Slovakia, 21-27.
64. Xue, J. and Øye, H.A., Light Metals 1999, 247-253.
65. Zhang, X.F., McLean, A. and Sommerville, I.D., Steelmaking conference proceedings, Washington, April 1991, pp. 659-662.